

抗がん剤耐性ががん細胞に対する耐性克服薬の開発と標的療法

朝 倉 正

東京慈恵会医科大学総合医科学研究センターアイソトープ実験研究施設

DEVELOPMENT OF THE REVERSAL DRUG FOR THE ANTICANCER DRUG-RESISTANT CELLS, AND TARGET CHEMOTHERAPY

Tadashi ASAKURA

Radioisotope Research Facilities, Research Center for Medical Sciences, The Jikei University School of Medicine

A conjugate of doxorubicin (DXR) with bovine serum albumin (BSA-DXR), which reversed multidrug resistance (MDR), exhibited potent cytotoxicity with the degraded active adducts with a molecular weight of approximately 2 to 3 kDa of BSA-DXR by lysosomal breakdown. Moreover, DXR conjugated to glutathione (GSH-DXR) with rapid intracellular accumulation without efflux improved the cytotoxicity against MDR cells. The GSH-DXR exhibited potent cytotoxicity against both DXR-sensitive cells and DXR-resistant cells, and the treatment with GSH-DXR caused cytochrome c to be released from mitochondria to the cytosol following potent activation of caspase 3 and caspase 9 by typical DNA fragmentation. This apoptosis was regulated by the c-Jun N-terminal kinase (JNK)-signaling pathway. The glutathione S-transferase (GST)-placental (P) type of GST isozyme was expressed in MDR cells, and active GST-P suppressed the JNK-signaling pathway by binding to JNK. Therefore, inhibition of GST-P activity by GSH-DXR induced apoptosis through liberation of the JNK-signaling pathway. To study the efficacy of a CD147-targeting agent on CD147-expressing carcinoma cells, we investigated the effect of GSH-DXR encapsulated in anti-CD147 antibody-labeled polymeric micelles (aCD147ab-micelles) in terms of specific accumulation and cytotoxicity in CD147-expressing human carcinoma cells. Specific accumulation of the aCD147ab-micelles in the CD147-expressing cells was observed. The GSH-DXR encapsulated in aCD147ab-micelles expressed specific cytotoxicity against these carcinoma cells. The target chemotherapy of GSH-DXR encapsulated in aCD147ab-micelles on CD147-expressing carcinoma cells was suggested to be effective. However, proteasome inhibitor has highly anticipated efficacy as an anticancer drug. We established proteasome inhibitor-resistant cancer cells that acquired invasiveness and induced epithelial-mesenchymal transition (EMT). In these cells up-regulation of zinc finger E-box-binding homeobox 1 (ZEB1) was induced via suppression of the micro RNA (miR)-200 family following suppression of E-cadherin, and the miR-200 family was placed upstream of ZEB1 to regulate the expression.

(Tokyo Jikeikai Medical Journal 2016;131:1-18)

Key words : multidrug resistance, glutathione S-transferase-placental, c-Jun N-terminal kinase, apoptosis, proteasome inhibitor, epithelial-mesenchymal transition, miRNA

I. はじめに

がんの化学療法において、抗がん剤の長期投与や化学療法後の再発時にしばしば抗がん剤に対して耐性を獲得することが知られている^{1) 2)}。ドキソルビシン (DXR) を代表とするアントラサイ

クリン系抗がん剤に対して薬剤耐性を獲得した細胞は、多くの場合P糖タンパク質 (Pgp) の過剰発現が観察される^{1) 2)}。PgpはATP binding cassette (ABC) スーパーファミリーに属する分子MDR/ABC B1で、分子量180kD、12回膜貫通タンパク質であり、ATP依存的に薬剤を細胞外に汲み出す

ポンプである^{3) 4)}。耐性を克服するために使用されることがあるPgpの阻害剤ベラパミルはカルシウムチャンネル阻害剤でもあり、心毒性などの副作用が問題となる⁵⁾⁻⁹⁾。そこで、試みられたのがPgpで汲み出せないように抗がん剤をタンパク質で修飾して高分子化することであった¹⁰⁾⁻¹²⁾。さらに、高分子化DXR由来の殺細胞効果発現分子を同定するために、細胞内薬物動態の検索から非常に強い殺細胞効果を有するグルタチオン(GSH)結合DXR (GSH-DXR) が得られた¹³⁾⁻¹⁶⁾。GSHの複合体が効果発現に関与することから、Glutathione S-transferase (GST) への作用が考えられる。GSTは脂溶性の薬剤にGSHを抱合結合し親水性分子として体外への排出を促す酵素であり、数種のアイソザイムが知られていて、中でも胎盤型GST (GST-P) が薬剤耐性に関与することが知られている¹⁷⁾⁻²⁰⁾。また、c-Jun N-terminal kinase (JNK) の活性化によりアポトーシスが誘導されること²¹⁾⁻²⁵⁾、GST-PがJNKに結合することでJNKシグナルを抑制することも報告されている²⁶⁾⁻³³⁾ので、GSH-DXRによる強い殺細胞効果およびアポトーシスの発現機序を解明していく³⁴⁾⁻³⁶⁾。また、GSH-

DXRを利用してイムノリポソームおよび、イムノミセルによるターゲティング療法の有効性を検討する。

最近、新規抗がん剤としてプロテアソーム阻害剤が利用されるようになってきたが、本薬剤に対して耐性を獲得した細胞が樹立された³⁷⁾³⁸⁾。また、薬剤耐性の獲得により上皮間葉転換 (EMT) が誘発されることが報告されている³⁹⁾⁻⁴⁵⁾ので、プロテアソーム阻害剤耐性細胞におけるEMT誘発の機序についても解明していく⁴⁶⁾。

II. ペプチド修飾 DXR による薬剤耐性克服

抗がん剤にタンパク質を修飾して高分子化することでPgpによる薬剤汲み出しを回避でき、薬剤耐性の克服が可能となることが大川らにより発表された¹⁰⁾⁻¹²⁾。ウシ血清アルブミン結合DXR (BSA-DXR) のラット腹水肝がん細胞AH66Pと同DXR耐性細胞AH66DRに対する殺細胞効果を調べると、BSA-DXRはAH66DRに対して耐性の克服を可能にするばかりか、AH66Pに対してDXR単剤よりも非常に強い殺細胞効果を発揮し、感受性細胞と耐性細胞で同程度の効果を有することが示された (Fig.1)。そこで、BSA-DXRは細

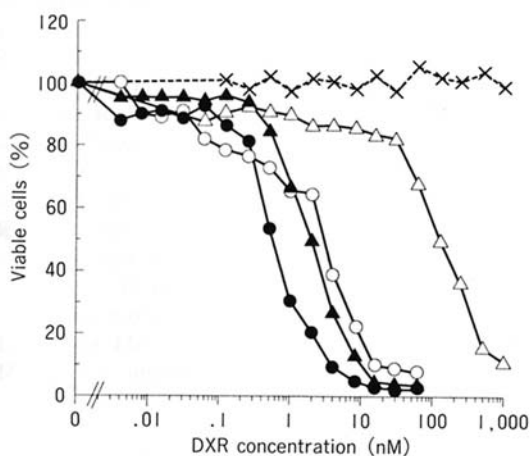


Fig.1. Cytotoxic effect of bovine serum albumin (BSA)-conjugated doxorubicine (DXR) (BSA-DXR) at the equivalent concentration of DXR on AH66 parent (DXR-sensitive) cell line (AH66P) and AH66 DXR-resistant cell line (AH66DR) cells examined using 3-(4,5-dimethylthiazol-2-yl)-2,5-diphenyl tetrazolium bromide (MTT) assay in terms of percentage of viable cells as compared with that of the control. AH66P; Δ : DXR, \circ : BSA-DXR AH66DR; \times : DXR, \blacktriangle : BSA-DXR, \bullet : BSA-DXR + verapamil (P-glycoprotein inhibitor)

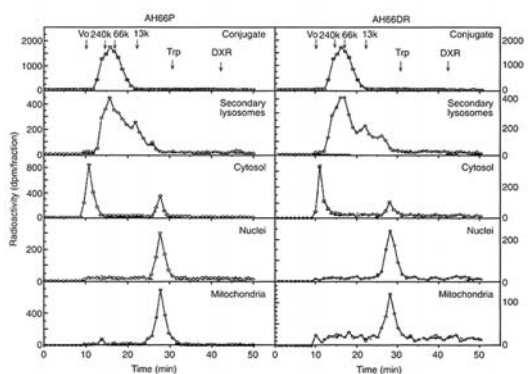


Fig.2. Estimation of molecular weight of the internalized DXR conjugate in the subcellular fraction after 24 hours treatment with BSA-DXR.

After 24 hours of treatment of both AH66P and AH66DR cells with BSA-DXR conjugate, molecular weight distribution of DXR compounds in secondary lysosomal, cytosolic, nuclear and mitochondrial fractions was estimated by high-performance liquid chromatography gel filtration (G3000SW column)¹³⁾. Vo: void volume; 240k: elution of 240kD polypeptide; 66k: elution of 66kD polypeptide; 13k: elution of 13kD polypeptide; Try: elution of trypsin; DXR: elution of DXR.

胞内に取り込まれた後、どのような分子として効果を発揮しているのかを調べるために、BSA-¹⁴C-

DXRを細胞に添加24時間後に各細胞内小器官を分画し、¹⁴C-化合物をゲルろ過で分画し細胞内薬物動態を検索した。二次リソソームで分解され、細胞質・核・ミトコンドリアに分子量1,000～3,000程度のペプチド-¹⁴C-DXR複合体として分散し、効果を発揮していることが示唆された^{13) 14)}(Fig.2)。そこで、種々のペプチドをDXRに結合させて殺細胞効果・耐性克服能・細胞内蓄積量を調べたところ、ペプチドとしてグルタチオン(GSH, ECG: γ -glutamyl-cysteinyl-glycine)に非常に強い効果が認められ(Fig.3)、耐性細胞内蓄積量も感受性細胞へのDXR蓄積量と同程度であった(Table 1)。ペプチドにグリシル・グリシル・グリシン(GGG)を用いた場合はほとんど効果がなかった。また、GSHのシステイン残基をアラニンやセリンに置換(EAG: γ -glutamyl-alanyl-glycine, ESG: γ -glutamyl-serinyl-glycine)したペ

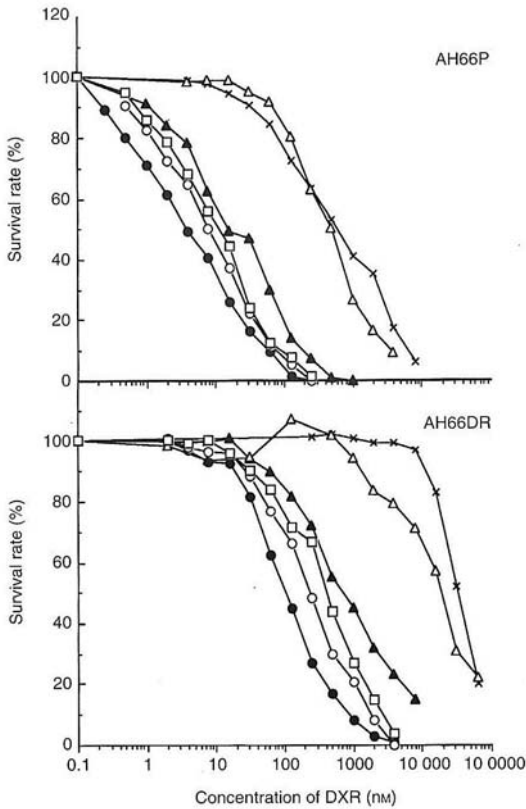


Fig.3. Cytotoxicity of DXR-peptide conjugates against AH66P and AH66DR cells examined with MTT assay in terms of the percentage of viable cells as compared with that of the control.
 × : DXR; ▲ : BSA-DXR; △ : glycyl-glycyl-glycine (GGG)-conjugated DXR (GGG-DXR); ● : glutathione (GSH)-conjugated DXR (GSH-DXR), ○ : γ -glutamyl-alanyl-glycine (EAG)-conjugated DXR (EAG-DXR), □ : γ -glutamyl-seryl-glycine (ESG)-conjugated DXR (ESG-DXR)³⁴⁾.

Table 1. The effect of verapamil on 50% growth-inhibitory concentration values for peptide-conjugated doxorubicin and the drug accumulation rates in AH66P and AH66DR cells

Drugs	GIC50 values (nM)			Drug accumulation rate (%)		
	AH66P	AH66DR	AH66DR	AH66P	AH66DR	AH66DR
	-VPL	-VPL	+VPL	-VPL	-VPL	+VPL
DXR	600	32,000	900	17.1	2.5	14.3
	± 90	± 15,000	± 190	± 2.0	± 0.8	± 2.3
BSA-DXR	30	600	40	11.3	9.7	12.1
	± 4.0	± 90	± 15	± 1.8	± 0.7	± 1.5
GGG-DXR	500	20,000	700	16.9	3.4	13.9
	± 70	± 5,000	± 210	± 1.9	± 1.1	± 1.3
GSH-DXR	3.5	80	16	15.0	13.4	14.0
	± 1.1	± 16	± 4	± 0.9	± 1.6	± 1.1
EAG-DXR	7.8	240	80	14.2	13.3	14.4
	± 1.5	± 40	± 10	± 2.6	± 2.1	± 2.0
ESG-DXR	10.0	300	90	13.9	13.1	14.1
	± 2.2	± 50	± 12	± 3.0	± 1.9	± 1.7

Incubation was performed in the presence or absence of 5 μ M verapamil (VPL). The 50% growth-inhibitory concentration (GIC50) values are expressed as equivalent concentrations of doxorubicin (DXR). Results are means \pm S.D. (4 or 5 independent experiments). The drug accumulation rate was expressed as intracellular DXR relative to DXR added to the medium during 24 hour of incubation. Abbreviations: AH66P, AH66 parent (DXR-sensitive) cell line; AH66DR, AH66 DXR-resistant cell line; BSA-DXR, bovine serum albumin-conjugated DXR; EAG-DXR, γ -glutamyl-alanyl-glycine-conjugated DXR; ESG-DXR, γ -glutamyl-seryl-glycine-conjugated DXR; GGG-DXR, glycyl-glycyl-glycine-conjugated DXR; GSH-DXR, glutathione-conjugated DXR.

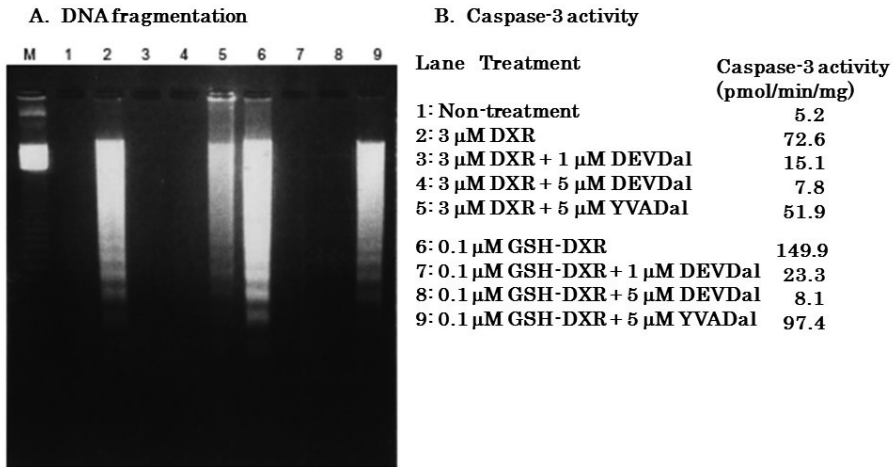


Fig.4. Induction of DNA fragmentation (A) and caspase-3 activation (B) by treatment of AH66P cells with DXR and GSH-DXR. The continuous treatment of the cells with 3 μM DXR or 0.1 μM GSH-DXR in the presence or absence of acetyl-aspartyl-glutamyl-valeryl-aspartyl-aldehyde (DEVDal, caspase-3 inhibitor) or acetyl-tyrosyl-valeryl-alanyl-aspartyl-aldehyde (YVADal, caspase-1 inhibitor) for 24 hours¹⁵.

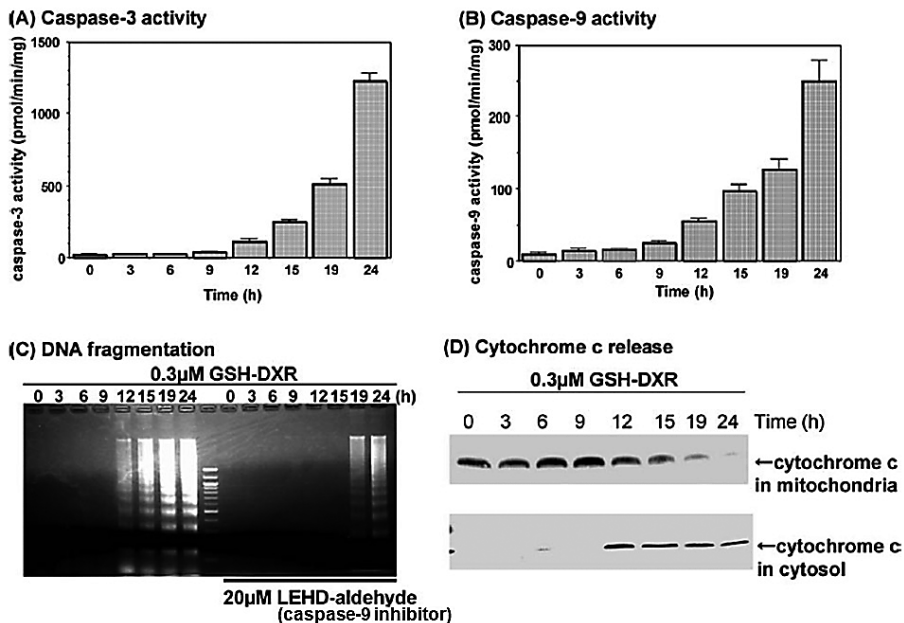


Fig.5. GSH-DXR (0.3 μM) induced activation of caspase-3 and caspase-9, fragmentation of DNA, and release of cytochrome c from the mitochondria to cytosol in AH66 cells. Caspase-3 (A) and caspase-9 (B) activation, DNA fragmentation (C), and cytochrome c release (D) in AH66 cells treated with 0.3 μM GSH-DXR for various periods of time were measured. DNA fragmentation in AH66 cells co-treated with 0.3 μM GSH-DXR and acetyl-leucyl-glutamyl-histidyl-aspartyl-aldehyde (LEHD-aldehyde) (20 μM), caspase-9 inhibitor was also measured. After treatment of AH66 cells with 0.3 μM GSH-DXR for various periods of time, the fragmented DNA was extracted with 1% Triton X-100 and separated by 2% agarose gel electrophoresis. The 100-base-pair DNA ladder marker was used as the standard DNA fragment. Caspase-3 and caspase-9 activities in the same extracts were determined with acetyl-aspartyl-glutamyl-valeryl-aspartyl- α -(4-methyl-coumaryl-7-amide) (DEVD-MCA) and acetyl-leucyl-glutamyl-histidyl-aspartyl- α -(4-methyl-coumaryl-7-amide) (LEHD-MCA) as substrates. Results are means \pm SD (3 independent experiments). Cytochrome c in both the mitochondrial and cytosolic fractions was detected by Western blot analysis using an anti-cytochrome c antibody. The amount of applied sample was 100 μg of protein in each lane³⁶.

プチドとの複合体では細胞内蓄積量はGSHを用いた場合と同程度であったが (Table 1), 殺細胞効果は3~5倍弱くなり, GSHのチオール基の存在が重要であることが示唆された^{16) 17)}.

III. GSH-DXR のアポトーシス誘導機序

GSH-DXRによる細胞障害性としてアポトーシス誘導能を調べるために, DXRおよびGSH-DXRをAH66P細胞に添加し24時間後にDNAおよびカスパーゼを抽出し, 断片化DNA およびCaspase-3活性を測定するとCaspase-3活性化およびDNA断片化が観察された. カスパーゼ-3阻害剤Asp-Glu-Val-Asp-aldehyde (DEVD-aldehyde) 処理により断片化DNAは消失したことから, カスパーゼ-3を介したアポトーシスを誘導していることは明らかであった¹⁶⁾ (Fig.4). アポトーシス経路にはデスレセプターを介した経路やミトコンドリアを介した経路などが知られている⁴⁷⁾⁻⁵⁶⁾ ので,

GSH-DXRによるアポトーシス誘発がどのような経路を介しているのかを調べると, ミトコンドリアからの細胞質へのシトクロムc放出, カスパーゼ-9活性化が観察され (Fig.5), さらにカスパーゼ-9の阻害剤Leu-Glu His-Asp-aldehyde (LEHD-aldehyde) 処理によりDNA断片化が抑制されたことから, ミトコンドリア経路であることが明らかとなった³⁵⁾.

IV. 耐性獲得因子GST-P変動に伴うアポトーシス調節

GSH-DXRの効果発現機序として, GSHがGSTの基質であること, GSTアイソザイムのGST-Pが薬剤耐性にかかわることが報告されている¹⁷⁾⁻²⁰⁾ こと, AH66Pに比べてAH66DRにおけるGST-P発現量が多いことから, GSH-DXRのGST-Pへの効果が考えられる. 事実, GSH-DXRはGST活性に対して阻害効果を示しそのIC50は1 μ Mで拮

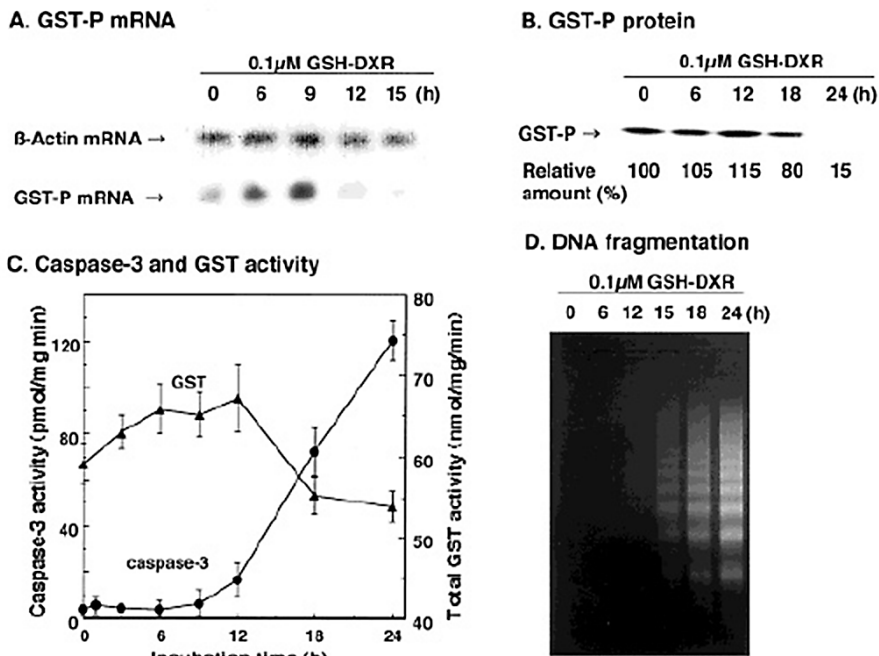


Fig.6. Time course of glutathione S-transferase-P (GST-P) messenger (m) RNA (A) and its protein expression (B), caspase-3 and GST activity (C), and DNA fragmentation (D) after treatment with GSH-DXR. After treatment of AH66P cells with 0.1 μ M GSH-DXR for various times, GST-P mRNA (Northern blot) and its protein (Western blot), caspase-3 activity (DEVD-MCA as a substrate), GST activity (1-chloro-2,4-dinitrobenzene (CDNB) and GSH as substrates), and DNA fragmentation (agarose gel electrophoresis) were measured as described previously (33-35). Relative amounts of GST-P protein were measured in a densitometer and compared with the nontreated control. Results are means \pm SD (3 independent experiments)³⁵⁾.

抗阻害であった。さらに、耐性細胞AH66DRをGSH-DXRで処理してGST-Pの発現の変動を調べると、遺伝子レベル・タンパク質レベルでその発現は強く抑制され³⁶⁾ (Fig.6A, B), それに伴ってカスパーゼ-3活性の上昇と断片化DNAの増加が観察された (Fig.6C, D)。

そこで、GST-P発現量の少ない感受性細胞AH66PにGST-Pを過剰発現させると、DXRに対する殺細胞効果はIC₅₀で260nMから1200nMへと薬剤感受性が低下した。さらに、耐性の獲得にGST-Pの活性中心の関与を調べるために、GST-Pの活性中心となるGSH結合部位や基質結合部位の変異体 (W38H, C47S) を感受性細胞に導入し過剰発現させ、DXRに対する殺細胞効果を調べた。野生型GST-P過剰発現による殺細胞効果の低下と比べ、いずれの変異体を発現させても殺細胞効果 (IC₅₀) に有意な差は認められなかった (Fig.7)。つまり、薬剤耐性には活性を持つGST-Pの発現が重要であることが明らかとなった³⁶⁾。

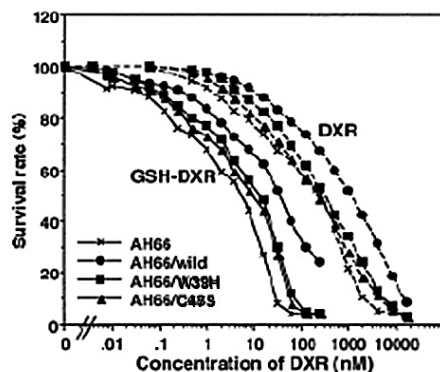
一方、GST-PはJNKに結合しmitogen-activated protein (MAP) キナーゼのシグナル伝達系に関与

する報告²⁵⁾⁻³²⁾があり、またJNK活性化によりアポトーシスが誘導される報告²⁰⁾⁻²⁴⁾があるので、GSH-DXRによるアポトーシス誘導におけるJNKとGST-Pとの相互作用について調べた。GSH-DXRで誘導されるアポトーシスはJNK阻害剤であるSP600125処理によりDNA断片化・カスパーゼ-3および-9活性化がともに抑制された (Fig.8)。また、GSH-DXR処理でJNKはリン酸化され、活性 (c-Junリン酸化) を示したが、JNK-ドミナントネガティブ (JNK/K55A, 活性中心の変異体) を発現させると、内在性JNKリン酸化が抑制されアポトーシスの指標であるカスパーゼ-3の活性化も抑制された。野生型JNKの過剰発現はJNKのリン酸化には影響なく、カスパーゼ-3の活性化はむしろ亢進していた。また、耐性細胞AH66DRにおいてJNKの免疫沈降によりGST-Pが共沈してきたことから、GST-PのJNKへの結合が観察された。しかし、AH66DR細胞をGSH-DXR処理してもJNKの免疫沈降によりGST-Pが共沈したことから、この結合はGSH-DXR処理によっても解離しなかった³⁵⁾。また、GSH-DXRによるアポトーシス誘発にはJNKと並

A. Expression of wild-type and site-directedly mutated GST-P



B. Cytotoxicity



IC₅₀ values (nM)

Cell line	DXR	GSH-DXR
AH66	260 ± 19	5 ± 0.30
AH66/vector	280 ± 35	5 ± 0.55
AH66/wild	1200 ± 95	32 ± 4.1
AH66/W38H	270 ± 22	14 ± 1.8
AH66/C47S	230 ± 31	10 ± 1.5

Fig.7. (A) Expression of transfected wild-type GST-P and site-directedly mutated GST-P (W38H: site directed mutant of 38th tryptophane to histidine, and C47S: site directed mutant of 47th cysteine to serine) in AH66 cells. (B) Cytotoxicities of DXR and GSH-DXR, and each 50% inhibitory concentration (IC₅₀) value in AH66 cells transfected with GST-P/wild, GST-P/W38H, and GST-P/C47S complementary (c) DNA. The expressed protein was recognized by an anti-GST-P antibody. The IC₅₀ values are means ± SD (3 independent experiments using different strains)³⁵⁾.

んでMAPキナーゼファミリーの一つである Extracellular Signal-regulated Kinase (ERK) の関与は認められなかった。

GSH-DXR処理によるJNKリン酸化および活性化 (c-Junリン酸化活性) は感受性細胞でも観察されたが、野生型GST-Pを発現させるとJNKはリン酸化されるが、JNK活性化は抑制 (c-Junリン酸化能の低下) されカパーゼ-3活性化も低下した。しかし、GST-Pの活性中心であるGSH結合部位や基質結合部位を変異させたもの (GST-P/W38H, GST-P/C47S) を導入し過剰発現させたとき、GST-P変異体は活性がなくてもJNKに結合するがJNKのリン酸化も基質c-Junをリン酸化する活性も阻害せず、アポトーシスの誘導も抑制しなかった³⁵⁾ (Fig.9)。つまり、JNK活性を抑制するためには活性を有するGST-Pが結合することが必要であり、結合してもGST活性がないとJNK活性を抑制できずアポトーシスが誘発された。このことから、GSH-DXRはJNKを活性

化するとともにGST-Pを阻害することで、JNK活性化を介したアポトーシスが誘発された。

そこで、GST-Pに活性はあるがJNKに結合しない場合について検討した。GST-PはそのC末端領域がJNKに結合するので、C末端領域を欠損したGST-P/ Δ C(194-209)、あるいは結合部位を変異したGST-P/R201Aを感受性細胞に過剰発現させたところ、JNKの免疫沈降によりGST-P/wildは共沈したがGST-P/ Δ C(194-209)、GST-P/R201Aはいずれもほとんど共沈せず、c-Junリン酸化活性も阻害されなかった。また、GST-P/ Δ C(194-209)にはGST活性はないが、GST-P/R201Aには活性があるので、JNK活性を抑制してアポトーシスを誘発を抑えるためには、活性のあるGST-PがJNKに結合する必要があることが明らかとなった³⁵⁾ (Fig.9)。

以上のことから、Fig.10に示すように、薬剤耐性を獲得しPgpおよびGST-Pを発現すると、GST-PはJNKに結合しその活性を阻害すること

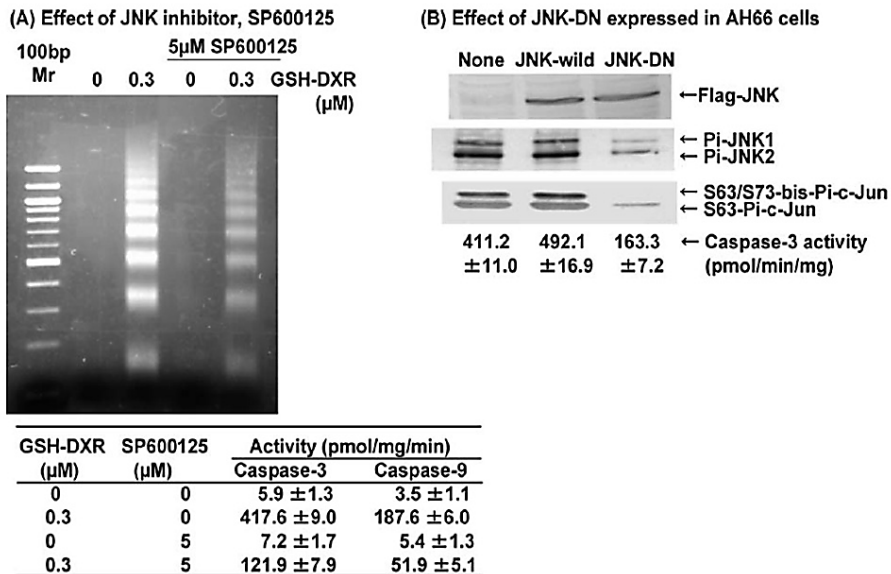


Fig.8. The effects of SP600125 (an inhibitor of c-Jun N-terminal kinase [JNK] activity) (A) and JNK-dominant negative (JNK-DN) (B) on GSH-DXR-induced apoptosis were measured. (A) After co-treatment of AH66 cells with 0.3 μ M GSH-DXR and 5 μ M SP600125 for 18 hours, the fragmented DNA was extracted with 1% Triton X-100 and separated by 2% agarose gel electrophoresis. The 100-base-pair DNA ladder was used as the standard DNA fragment. Caspase-3 and caspase-9 activities in the same extracts were determined with DEVD-MCA and LEHD-MCA as substrates. Results are means \pm SD (3 independent experiments). (B) After treatment of AH66 cells expressed with Flag-JNK/wild and Flag-JNK/K55A (site directed mutant of 55th lysine to alanine, JNK-DN) with 0.3 μ M GSH-DXR for 18 hours, activated JNK (phosphorylated-JNK [Pi-JNK]), JNK activity (phosphorylation of c-Jun [Pi-c-Jun]), and caspase-3 activity were measured. Expressed Flag-tagged JNK was determined with Western blot and anti-Flag antibodies. The Pi-JNK and Pi-c-Jun were detected with anti-phospho-JNK (183T and 185Y) and anti-phospho-c-Jun (63S) antibodies, respectively³⁶⁾.

でJNKを介したミトコンドリア経路のアポトーシスを抑制する。したがって、Pgpの薬剤汲み出しが回避でき、GST-P阻害が有効な耐性克服薬となりうるであろう。

V. GSH-DXRを利用したターゲティング療法の有効性

GSH-DXRは非常に強い殺細胞効果を有する薬剤であるので、標的治療に用いることにより、一層特異的効果が発揮できることが期待される。そこで、横山ら^{57) 58)}の開発したブロックコポリマーミ

セルを用いて検討した (Fig.11)。このミセルの特徴は血液滞留性の良いことで、リポソームよりも数倍優れており標的治療に効果が期待できる^{57) 58)}。

また、標的に選んだCD147 (EMMPRIN, Basigin)は分子量58kD、メタロプロテアーゼ産生を亢進し腫瘍悪性化に関与する膜貫通糖タンパク質であり⁵⁸⁾⁻⁶⁰⁾、Fig.12に示すように、正常組織では腎、乳房、前立腺に発現が認められるが、他の臓器にほとんど発現はなく、がん化に伴い高発現するので、標的として効果が期待できる⁶¹⁾⁻⁶⁵⁾。そこで、抗CD147抗体を作製しGFPとともにミセル表面に結合し二重標識した (Fig.11)。コントロール

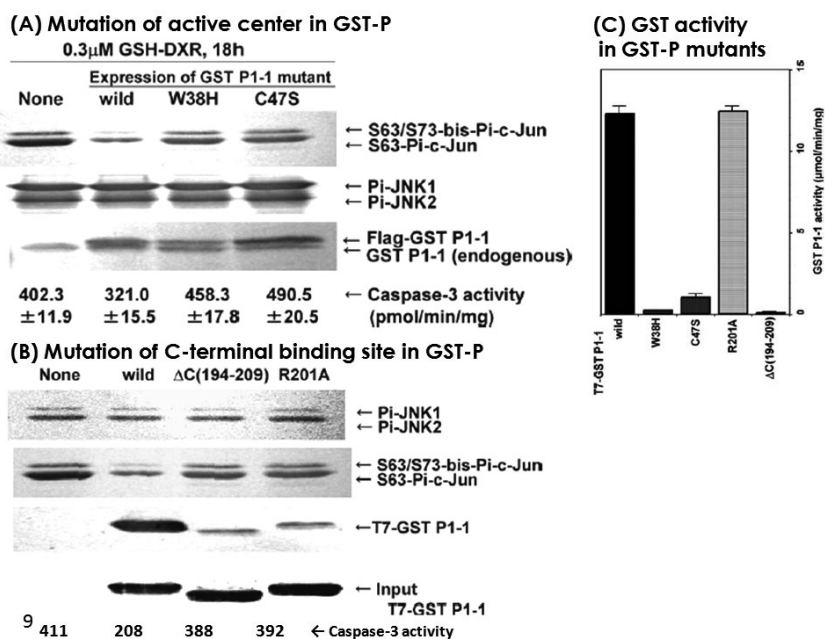


Fig.9. Activation of JNK (Pi-JNK and Pi-c-Jun) in AH66 cells expressed with Flag-GST-P/wild, Flag-GST-P/W38H, Flag-GST-P/C47S, T7-GST-P/ΔC(194-209) (C-terminal deletion), and T7-GST-P/R201A (site directed mutant of 201th arginine to alanine). (A) Activation of JNK in AH66 cells expressed with Flag-GST P1-1/wild, Flag-GST P1-1/W38H, and Flag-GST P1-1/C47S by treatment with GSH-DXR. Activation of JNK (Pi-c-Jun and Pi-JNK), binding of expressed Flag-GST P1-1/wild, Flag-GST P1-1/W38H, and Flag-GST P1-1/C47S to the JNK molecule and activity of caspase-3 in AH66 transfectant cells treated with 0.3 µM GSH-DXR for 18 hours were measured. Pi-JNK, Pi-c-Jun, endogenous GST P1-1 and expressed Flag-GST P1-1/wild, and Flag-GST P1-1/W38H and Flag-GST P1-1/C47S bound to the JNK molecule were analyzed by Western blot analysis using anti-phospho-JNK (183T and 185Y), anti-phospho-c-Jun (63S), and anti-GST-P antibodies, respectively. Caspase-3 activity was determined using DEVD-MCA as a substrate. (B) Effects of C-terminal deletion mutant of GST P1-1 (T7-GST P1-1/ΔC [194-209]) and C-terminal mutated GST P1-1 (T7-GST P1-1/R201A) on binding and activity of JNK. The JNK activity was expressed as Pi-c-Jun. Extracts from AH66 cells irradiated with ultraviolet light were used as the enzyme source. JNK (including the active form) purified by affinity precipitation (binding to c-Jun fusion resin) was reacted with 100 µM ATP in the presence or absence of T7-GST P1-1/wild or the mutants. After the resin was washed, Pi-c-Jun, Pi-JNK (active form of JNK), JNK and T7-GST P1-1 were measured by Western blot analysis using anti-phospho-c-Jun (63S), anti-phospho-JNK (183T and 185Y), and anti-T7 antibodies, respectively. (C) GST activity in T7-tagged GST P1-1/wild and its mutants (T7-GST P1-1/W38H and T7-GST P1-1/C47S). The activity was determined with 1 mM GSH and 1 mM CDNB as substrates. T7-GST P1-1/wild, T7-tagged wild type GST P1-1; T7-GST P1-1/ΔC(194-209), C-terminal deletion mutant; T7-GST P1-1/R201A, site-directed mutation of the C-terminal region; T7-GST P1-1/W38H and T7-GST P1-1/C47S, site-directed mutation of the active center. Results are means ± SD (3 independent experiments)³⁹⁾.

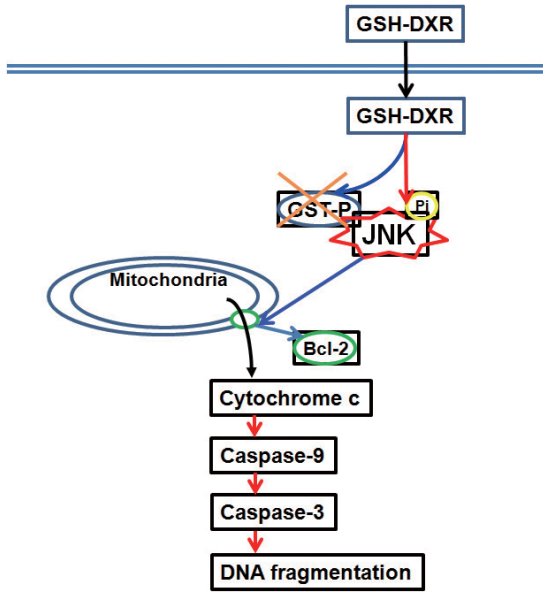


Fig.10. Proposed model for apoptosis induction by GSH-DXR. GSH-DXR induced activation of JNK according to JNK phosphorylation and GST-P inhibition. Bcl-2 phosphorylated by active JNK was dissociated from mitochondrial membrane, and cytochrome c was released through the produced pore by the dissociation from mitochondria to cytosol. DNA was fragmented by following activation of caspase-9 and caspase-3.

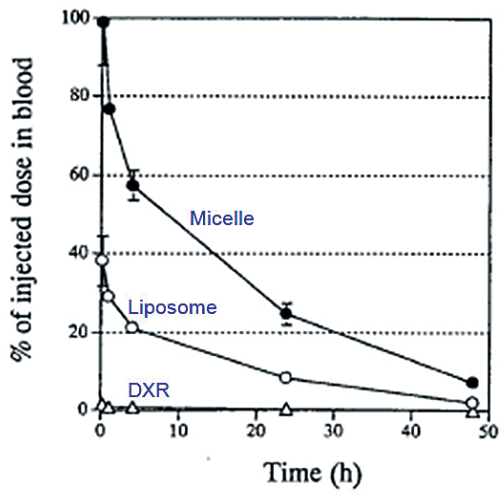
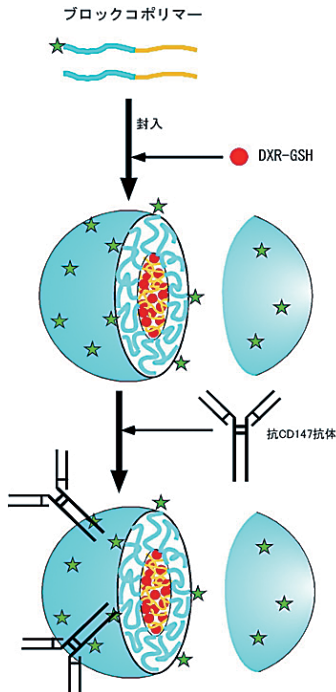


Fig.11. (A) Preparation of anti-CD147 antibody-labeling polymeric micelles (aCD147ab-micelles) encapsulated GSH-DXR. Star sign: Fluorescent Dye GFP. (B) DXR concentration in blood after intravenous injection. ● : polymeric micelles, ○ : liposomes, △ : DXR. ¹⁴C-labeled polymeric micelles or ¹⁴C-labeled DXR was injected into the tail veins of female mice (7 weeks old) at a volume of 0.1 ml/10 g body weight. The dose was either 10 mg/kg for ADR or 10 mg of the total amount of both physically entrapped ADR (intact) and the dimer/kg for the polymeric micelles. After defined time periods (15 minutes, 1, 4, 24, and 48 hours), mice were anesthetized with diethylether. Blood samples were collected from the right axillary artery. Total radioactivity in blood was calculated by assuming that the total blood volume was 2.18 ml/25 g of body weight.

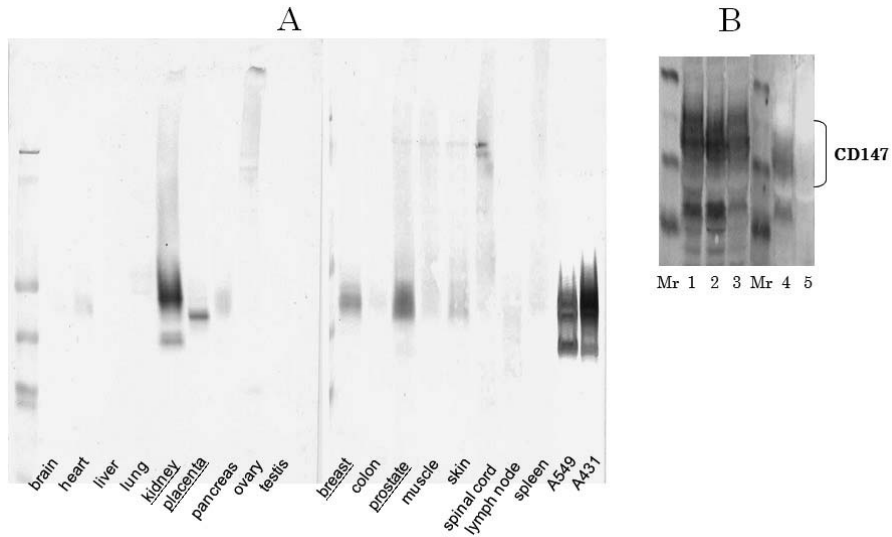


Fig.12. Expression of CD147 in human normal tissues (brain, heart, liver, lung, kidney, placenta, pancreas, ovary, testis, breast, colon, prostate, muscle, skin, spinal cord, skin, spinal cord lymph node, and spleen) and cancer cells (human alveolar basal epithelial cell A549 and human squamous carcinoma A431) (A), and several cancer cell lines (1: A431; 2: human ovarian carcinoma A2780; 3: human endometrial adenocarcinoma Ishikawa; 4: human prostate carcinoma PC3; and 5: CD147-knock down PC3) (B) by Western blot analysis with aCD147abs.

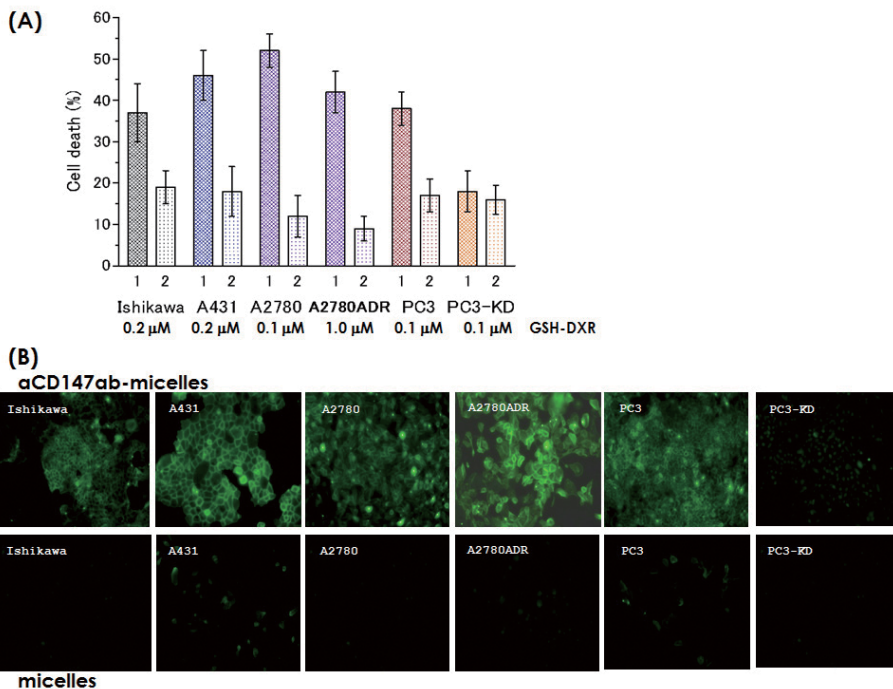


Fig.13. Cytotoxicity and accumulation of aCD147ab-micelles (for 1 hour of exposure) against several cells. 1: aCD147ab-micelles, 2: rabbit immunoglobulin G (IgG)-micelles. (A) Cytotoxicity of aCD147ab-micelles/GSH-DXR (for 1 hour of exposure) against Ishikawa, A431, A2780, A2780ADR, PC3, and PC3/KD (CD147 knock down) cells. (B) Accumulation of aCD147ab-micelles (upper panel) and control rabbit IgG-micelles (lower panel) for 0.5 hour of exposure in human carcinoma cells (A431, Ishikawa, A2780, and PC3). Accumulation of micelles was observed under fluorescent microscopy with Thermofisher Alexa 548 dye.

では抗CD147抗体の代わりにRabbit IgGを用いた。培養系で、GSH-DXRを内封したミセルを細胞に1時間暴露し、3日後にMTS assayによる生細胞数の測定から殺細胞効果を比較すると、抗CD147抗体標識により非常に有効な殺細胞効果が観察された (Fig.13)。さらに、抗CD147抗体標識によりGFPの集積が確認された (Fig.13)。CD147をノックダウンしたPC3-KDではRabbit IgGを標識した場合と有意な殺細胞効果は認められず、GFPの集積もなかったことから、CD147を標的としたターゲティング療法が期待される。このターゲティングの効果は、抗CD147抗体

を標識したイムノリポソームを用いても同様の集積が確認されたが、GSH-DXRの内封量が少なかったため殺細胞効果がミセルの場合よりも弱かったことから、ミセル利用の有効性が期待された。

VI. プロテアソーム阻害剤耐性獲得による EMT 誘発機序

最近、新規抗癌剤としてプロテアソーム阻害剤が認められ利用されるようになってきた⁶⁶⁾⁻⁸⁰⁾。多発性骨髄腫治療に用いられるボルテゾミブ (ベ

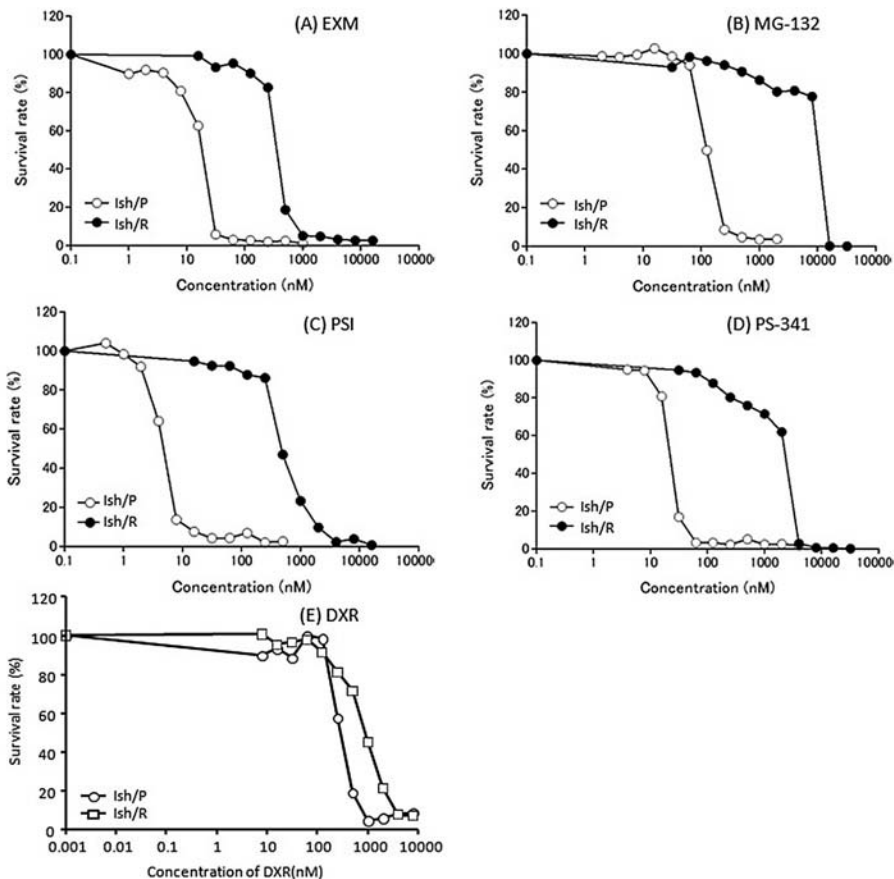


Fig.14. Cytotoxicity of some proteasome inhibitors against Ishikawa (IshP) and epoxomicin (EXM)-resistant Ishikawa (IshR) cells. Cytotoxicity of EXM (A), *N*-(Benzoyloxycarbonyl)leucylleucylleucinal (MG-132) (B), *N*-[(Phenylmethoxy)carbonyl]-L-isoleucyl-L- α -glutamyl-*tert*-butyl ester-*N*-[(1*S*)-1-formyl-3-methylbutyl]-L-alaninamide (PSI) (C), [(1*R*)-3-methyl-1-((2*S*)-3-phenyl-2-[(pyrazin-2-ylcarbonyl)amino]propanoyl)amino]butyl]boronic acid (PS-341, Bortezomib) (D), and DXR (E) against Ishikawa and Ish/EXM cells. The cells were cultured continuously for 96 hours at 37°C in a 48-well culture plate with 0.5 ml of EXM, MG-132, PSI, PS-341, or DXR containing growth medium at graded equivalent concentrations of each drug. After incubation, 3-(4,5-dimethylthiazol-2-yl)-5-(3-carboxymethoxyphenyl)-2-(4-sulfophenyl)-2H-tetrazolium (MTS reagent) was added to each well and measured at 490 nm⁴⁶⁾.

ルケイド) がその代表である。このプロテアソーム阻害剤に対しても、いくつかの種類のがん細胞で薬剤耐性の獲得が観察された^{37) 38)}。そして、この耐性の獲得に伴い上皮間葉転換 (EMT) が誘発されることを見出し、転移・浸潤能が増すことでより一層の悪性化を伴うことが考えられたので、EMT 誘発機序について検討した。

子宮内膜がん細胞 Ishikawa cells においてプロテアソーム阻害剤エポキシソミン (EXM) に耐性を獲得した細胞を樹立した^{37) 38)}。本細胞は EXM だけでなく MG-132, PSI, PS-341 など多くのプロテアソーム阻害剤に対しても交差耐性を示した⁴⁶⁾ (Fig.14) が, DXR には耐性を示さずプロテアソーム阻害剤に特異的であった。そして, 上皮系のマーカーである E-カドヘリン (CDH1) 発現が消失し, 間葉系のマーカーであるビメンチン (VIM) の発現亢進が観察された⁴⁶⁾ (Fig15A)。さらに, ボイデンチャンバーを用いて浸潤した細胞を染色してその浸潤能を調べると, 明らかに耐性細胞で亢進しており, EMT が誘発されていることがわかった⁴⁶⁾ (Fig.15B)。CDH1 は転写抑制因子によりその発現が抑制されることが知られており, ここで

も ZEB1, ZEB2, Slug, Snail, Twist が耐性獲得に伴いその発現が増加し, これらの因子が関与していることが示唆された (Fig.15A)。そこで, 耐性細胞の各転写抑制因子の発現をそれぞれ siRNA で抑制したところ, ZEB1 の発現を抑制することで CDH1 の発現が遺伝子・タンパク質レベルで回復し, ZEB2 の抑制ではわずかながらの回復が, その他の因子はほとんど効果がなかった⁴⁶⁾ (Fig.16)。

最近, 多くの遺伝子発現の制御がマイクロ RNA (miRNA) によって行われているといわれ, EMT 関連でも miRNA の関与している報告がある^{81) -88)} ので, その 24 種類について調べてみたところ, miR200a, miR200b, miR200c, miR141 の発現が耐性細胞で消失していた⁴⁶⁾ (Fig.17)。これら 4 つの miRNA は miR200 family で塩基配列の相対性が高いものである。また, siRNA により耐性細胞の ZEB1 をノックダウンしても, 消失している miR200 family の発現は回復せず, ZEB2 のノックダウンでは miR200 family の発現は一部回復したので, miR200 family は ZEB1 の上流に位置し, ZEB2 は相互にフィードバック調節していることも考えられた⁸⁴⁾ (Fig.18)。そこで, miR200 family

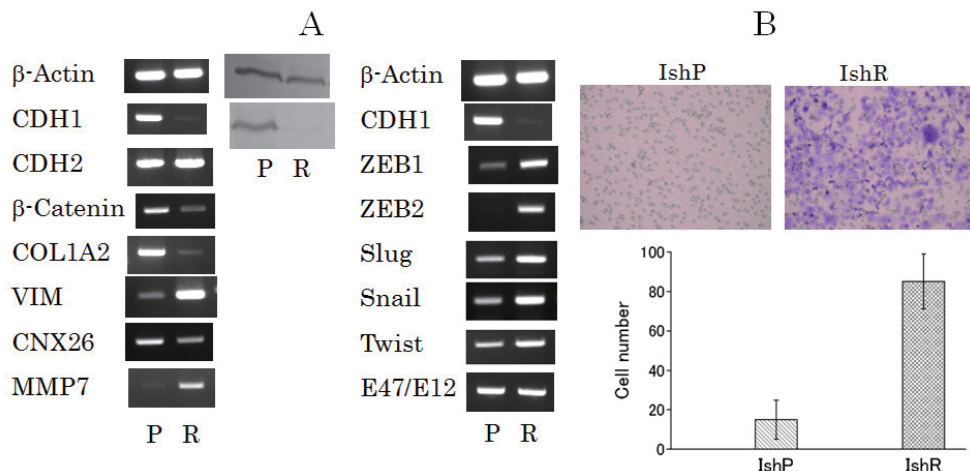


Fig.15. (A) Expression of mRNA level of epithelial marker (cadherin 1 [CDH1], collagen 1A2 [COL1A2], connexin 26 [CNX26], beta-catenin 1: [CNTB1]), mesenchymal marker (vimentin [VIN], cadherin 2 [CDH2], fibronectin 1 [FN1]), and transcriptional repressors (ZEB [zinc finger E-box-binding homeobox]1, ZEB2, Slug, Snail, Twist, E47/E12), and of the protein level of E-cadherin and ZEB1 by acquirement of EXM-resistance. P, Ish/P; R, Ish/R cells. (B) Cell migration of IshP and Ish/R. A total of 1×10^5 cells were plated in the top chamber onto a Matrigel-coated membrane (24-well insert; pore size, $8 \mu\text{m}$, Greiner Japan). Each well was coated freshly with Matrigel (60 mg) before the invasion assay. Cells were plated in medium without serum and growth factors, and medium supplemented with serum was used in the lower chamber. The cells were incubated for 24 hours, and cells that did not invade through the pores were removed with a cotton swab. Cells on the lower surface of the membrane were fixed with methanol and stained with crystal violet. The number of cells invading through the membrane was counted under a light microscope (3 random fields per well)⁴⁶⁾.

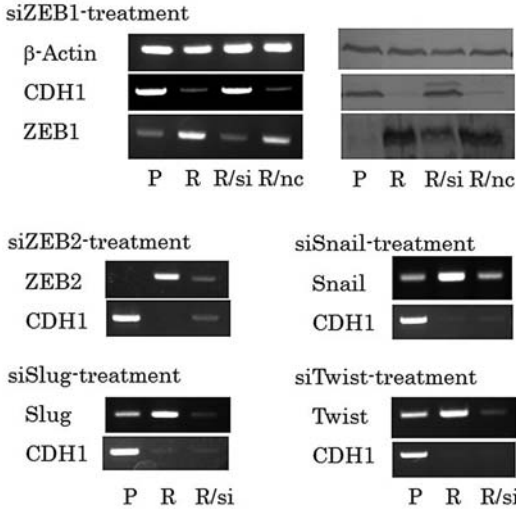


Fig.16. Effect of the knock-down of transcriptional repressors (ZEB1, ZEB2, Snail, Slug, and Twist) by transfection with their respective small interfering (si) RNA on E-cadherin expression. R/si, R/nc: treatment of Ish/R cells (R) with siRNA for each transcriptional repressor and noncoding RNA, respectively. P, Ish/P cells⁴⁶⁾.

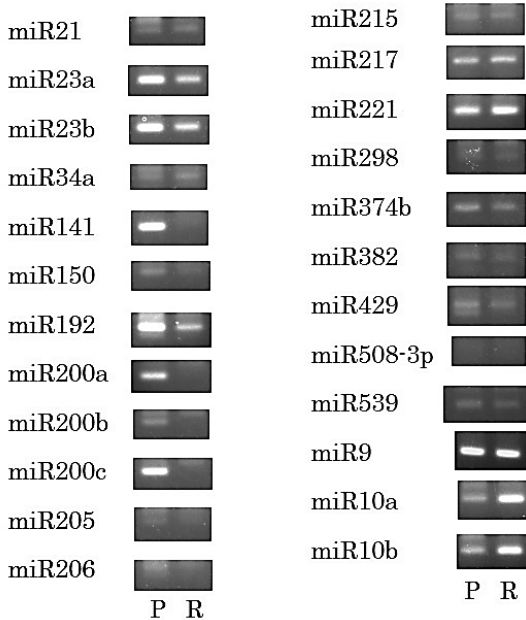


Fig.17. Comparison of the expression of several miRNAs in Ish/P (P) and Ish/R cells (R). MiRNA level was measured using the QuantiMir kit. Briefly, miRNA was tailed with polyA and annealed with oligo-dT adaptor, and then first-strand cDNA was created by reverse transcription. The expression level of miRNA was measured with the polymerase chain reaction using the obtained cDNA as a template, and the primers used were: forward, miRNA-specific sequence; reverse, universal reverse primer into the oligo-dT adaptor sequence⁴⁶⁾.

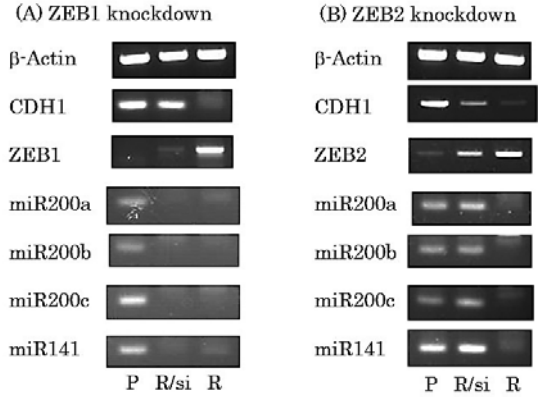


Fig.18. Effect of ZEB1 (A) and ZEB2 (B) knockdown by each siRNA on miR200 family expression. P, Ishikawa cells; R, Ish/EXM cells; R/si, Ish/EXM treated with siRNA for ZEB1 or ZEB2. CDH1 and ZEB1 mRNA were determined with reverse transcriptase-polymerase chain reaction. The miR 200 family was measured with the QuantiMir kit⁴⁶⁾.

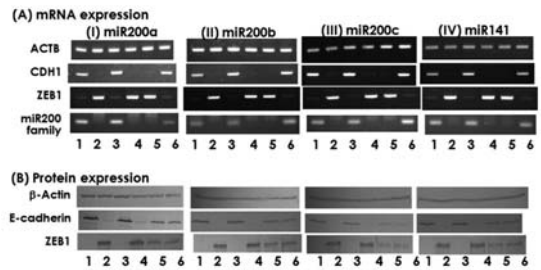


Fig.19. Effect of regulation of miR200 family expression on the expression of ZEB1 and CDH1 (E-cadherin) mRNA (A) and protein (B) in Ishikawa and Ish/EXM cells by transfection with the anti-miR200 family and the pre-miR200 family, respectively. Lane 1, Ishikawa cells; lane 2, Ish/EXM cells; lane 3, noncoding miR-transfected Ishikawa cells; lane 4, noncoding miR-transfected Ish/EXM cells; lane 5, anti-miR200 family (miR200a, miR200b, miR200c and miR141, respectively)-transfected Ishikawa cells; lane 6, pre-miR200 family (miR200a, miR200b, miR200c, and miR141, respectively)-transfected Ish/EXM cells⁴⁶⁾.

の発現量を anti-miRNA および pre-miRNA を用いて調節した。Lane 1 の miR200 の発現している感受性細胞の miR200 を anti-miR200 でノックダウンすると、Lane 5 のように ZEB1 の発現と CDH1 の消失が観察され、miR200 の消失している Lane 2 の耐性細胞に miR200 を pre-miR200 で発現させると、Lane 6 のように ZEB1 が消失し CDH1 の発現が回復した⁴⁶⁾ (Fig19)。タンパク質レベルでも同様の結果となり、miR200 family が ZEB1 の上流に位置することが明らかとなった。結果には示していないが、ZEB2 についても同様な結果が得られ相互に調節されていることが示唆された。

以上のことから、miR200 family が ZEB1, ZEB2 の発現を制御し、それに伴い CDH1 の発現が調節されていた。つまり、感受性細胞では miR200 family が発現しているため ZEB1, ZEB2 共にその発現は抑制され、CDH1 は発現している。しかし、耐性を獲得すると miR200 family の発現は消失し、ZEB1, ZEB2 共にその抑制が解除され発現が回復・

亢進する結果、CDH1 の発現を抑制し EMT を誘発することが示唆された^{89) 90)} (Fig.20)。

今後、耐性の獲得による miR200 family の発現抑制の機構について検討することで、より有効な治療法が解明できるであろう。

著者の利益相反 (conflict of interest : COI) 開示 :

本論文の研究内容に関連して特に申告なし

文 献

- 1) Riordan JR, Deuchars K, Kartner N, Alon N, Trent J, Ling V. Amplification of P-glycoprotein genes in multidrug-resistant mammalian cell lines. *Nature*. 1985; 316: 817-9.
- 2) Endicott JA, Ling V. The biochemistry of P-glycoprotein-mediated multidrug resistance. *Annu Rev Biochem*. 1989; 58: 137-71.
- 3) Benet LZ. The drug transporter-metabolism alliance: uncovering and defining the interplay. *Mol Pharm*. 2009; 6: 1631-43.
- 4) Baguley BC. Multidrug resistance in cancer. *Methods Mol Biol*. 2010; 596: 1-14.
- 5) Tsuruo T, Iida H, Tsukagoshi S, Sakurai Y. Increased accumulation of vincristine and adriamycin in drug-resistant P388 tumor cells following incubation with calcium antagonists and calmodulin inhibitors. *Cancer Res*. 1982; 42: 4730-3.
- 6) Fitzgerald DJ, Willingham MC, Cardarelli CO, Hamada H, Tsuruo T, Gottesman MM, et al. A monoclonal antibody-Pseudomonas toxin conjugate that specifically kills multidrug-resistant cells. *Proc Natl Acad Sci USA*. 1987; 84: 4288-92.
- 7) Twentyman PR, Fox NE, White DJG. Cyclosporin A and its analogues as modifiers of adriamycin and vincristine resistance in a multi-drug resistant human lung cancer cell line. *Br J Cancer*. 1987; 56: 55-7.
- 8) Tsuruo T, Hamada H, Sato S, Heike Y. Inhibition of multidrug resistant human tumor growth in athymic mice by anti-P-glycoprotein monoclonal antibodies. *Jpn J Cancer Res*. 1989; 80: 627-31.
- 9) Chen AY, Yu C, Potmesil M, Wall ME, Wani MC, Liu LF. Camptothecin overcomes MDR 1-mediated resistance in human KB carcinoma cells. *Cancer Res*. 1991; 51: 6039-44.
- 10) Hatano T, Ohkawa K, Matsuda M. Cytotoxic effect of the protein doxorubicin conjugates on the multidrug-resistant human myelogenous leukemia cell line, K562, in vitro.

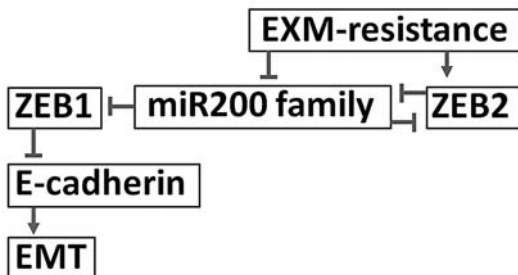


Fig.20. Proposed model for a molecular link between ZEB1, ZEB2, miR200 family, and E-cadherin. In initial studies, an inverse correlation between the miR200 family and ZEB1 was established in Ishikawa and Ish/EXM cells. Suppression of ZEB1 by the miR-200 family resulted in enhanced expression of E-cadherin and acquisition of an epithelial phenotype. During the induction of epithelial-mesenchymal transition (EMT) in Ish/EXM cells with acquirement of EXM-resistance, the miR200 family and E-cadherin were repressed in parallel with an increase in ZEB1 expression. The ability to induce EMT was dependent upon suppression of the miR200 family and induction of ZEB1 expression. Conversely, a mesenchymal-epithelial transition (MET) could be induced by expression of the miR200 family in cells that were originally mesenchymal in nature. These results confirm that the miR200 family represses ZEB1 expression and consequently inhibits the progression of EMT by establishing and maintaining an epithelial phenotype. The suppression of ZEB1 expression by the miRNA200 family is direct and occurs as a result of the miRNA binding to the 8 and the 9 sites in the 3' untranslated region of ZEB1 (and ZEB2) mRNA⁸⁸⁾⁸⁹⁾.

- Tumor Biol. 1993; 14: 288-94
- 11) Ohkawa K, Hatano T, Tsukada Y, Matsuda M. Chemotherapeutic efficacy of the protein-doxorubicin conjugates on multidrug resistant rat hepatoma cell line in vitro. *Br J Cancer*. 1993; 67: 274-8.
 - 12) Ohkawa K, Hatano T, Yamada K, Joh K, Takada K, Tsukada Y, et al. Bovine serum albumin-doxorubicin conjugate overcomes multidrug resistance in a rat hepatoma. *Cancer Res*. 1993; 53: 4238-42
 - 13) Takahashi N, Asakura T, Ohkawa K. Pharmacokinetic analysis of protein-conjugated doxorubicin (DXR) and its degraded adducts in DXR-sensitive and -resistant rat hepatoma cells. *Anti-Cancer Drugs*. 1996; 7: 2958-67.
 - 14) 高橋直人, 朝倉正, 大川清, 福田佳三, 青木照明. ウシ血清アルブミン結合Doxorubicinの細胞内薬物動態と多剤耐性克服. *癌と化療*. 1997; 24: 87-92.
 - 15) Asakura T, Takahashi N, Takada K, Inoue T, Ohkawa K. Drug conjugate of doxorubicin with glutathione is a potent reverser of multidrug resistance in rat hepatoma cells. *Anti-Cancer Drugs*. 1997; 8: 199-203.
 - 16) Asakura T, Sawai T, Hashidume Y, Ohkawa Y, Yokoyama S, Ohkawa K. Caspase-3 activation during doxorubicin conjugated with glutathione-mediated apoptosis. *Br J Cancer*. 1999; 80: 711-5.
 - 17) Batist G, Tulpule A, Sinha BK, Katki AG, Myers CE, Cowan KH. Overexpression of a novel anionic glutathione transferase in multidrug resistant human breast cancer cells. *J Biol Chem*. 1986; 261: 15544-9.
 - 18) Black SM, Beggs JD, Hayes JD, Bartoszek A, Muramatsu M, Sasaki M, et al. Expression of human glutathione S-transferases in *Saccharomyces cerevisiae* confers resistance to the anticancer drugs adriamycin and chlorambucil. *Biochem J*. 1988; 268: 309-15.
 - 19) Lewis AD, Hayes JD, Wolf CR. Glutathione and glutathione dependent enzymes in adenocarcinoma cell lines derived from a patient before and after the onset of drug resistances: intrinsic differences and cell cycle effects. *Carcinogenesis*. 1988; 9: 1283-7.
 - 20) Tew KD. Glutathione associated enzymes in anticancer drug resistance. *Cancer Res*. 1994; 54: 4313-20.
 - 21) Xia Z, Dickens M, Raingeaud J, Davis RJ, Greenberg ME. Opposing effects of ERK and JNK-p38 MAP kinases on apoptosis. *Science*. 1995; 270: 1326-31.
 - 22) Chen YR, Wang X, Templeton D, Davis RJ, Tan TH. The role of c-Jun N-terminal kinase (JNK) in apoptosis induced by ultraviolet c and gamma radiation. Duration of JNK activation may determine cell death and proliferation. *J Biol Chem*. 1996; 271: 31929-36.
 - 23) Guo YL, Baysal K, Kang B, Yang LJ, Williamson JR. Correlation between sustained c-Jun N-terminal protein kinase activation and apoptosis induced by tumor necrosis factor- α in rat mesangial cells. *J Biol Chem*. 1998; 273: 4027-34.
 - 24) Sanchez-Perez I, Murguia JR, Perona R. Cisplatin induces a persistent activation of JNK that is related to cell death. *Oncogene*. 1998; 16: 533-40.
 - 25) Javelaud D, Besanc, on F. NF- κ B activation results in rapid inactivation of JNK in TNF α -treated Ewing sarcoma cells: a mechanism for the anti-apoptotic effect of NF- κ B. *Oncogene*. 2001; 20: 4365-72.
 - 26) Shim J, Lee H, Park J, Kim H, Choi EJ. A non-enzymatic p21 protein inhibitor of stress-activated protein kinases. *Nature*. 1996; 381: 804-6.
 - 27) Adler V, Yin Z, Fuchs SY, Benezra M, Rosario L, Tew KD, et al. Regulation of JNK signaling by GSTp. *EMBO J*. 1999; 18: 1321-34.
 - 28) Shim J, Park HS, Kim MJ, Park J, Park E, Cho SG, et al. Rb protein downregulates the stress-activated signals through inhibiting c-Jun N-terminal kinase/stress-activated protein kinase. *J Biol Chem*. 2000; 275: 14107-11.
 - 29) Yin Z, Ivanov VN, Habelhah H, Tew KD, Ronai Z. Glutathione S-transferase *p* elicits protection against H₂O₂-induced cell death via coordinated regulation of stress kinases. *Cancer Res*. 2000; 60: 4053-7.
 - 30) Park HS, Lee JS, Huh SH, Seo JS, Choi EJ. Hsp72 functions as a natural inhibitory protein of c-Jun N-terminal kinase. *EMBO J*. 2001; 20: 446-56.
 - 31) Wang T, Arifoglu P, Ronai Z, Tew KD. Glutathione S-transferase P1-1 (GSTP1-1) inhibits c-Jun N-terminal kinase (JNK1) signaling through interaction with the c terminus. *J Biol Chem*. 2001; 276: 20999-1003.
 - 32) Adler V, Pincus MR. Effector peptides from glutathione-S-transferase-pi affect the activation of jun by jun-N-terminal kinase. *Ann Clin Lab Sci*. 2004; 34: 35-46.
 - 33) Chie L, Adler V, Friedman FK, Chung D, Pincus MR. An effector peptide from glutathione-S-transferase-pi strongly and selectively blocks mitotic signaling by oncogenic ras-p21. *Protein J*. 2004; 23: 235-8.
 - 34) Asakura T, Ohkawa K, Takahashi N, Takada K, Inoue T, Yokoyama S. Glutathione-doxorubicin conjugate expresses potent cytotoxicity by suppression of glutathione S-transferase activity: comparison between doxorubicin-sensitive and -resistant rat hepatoma cells. *Br J Cancer*. 1997; 76: 1333-7.
 - 35) Asakura T, Hashizume Y, Tashiro K, Searashi Y, Ohkawa K, Nishihira J, et al. Suppression of GST-P by treatment with glutathione-doxorubicin conjugate induces potent apoptosis in rat hepatoma cells. *Int J Cancer*. 2001; 94: 171-7.

- 36) Asakura T, Sasagawa A, Takeuchi T, Shibata S, Marushima H, Mamori S, et al. Conformational change in the active center region of GST P1-1, due to binding of a synthetic conjugate of DXR with GSH, enhanced JNK-mediated apoptosis. *Apoptosis*. 2007; 12: 1269-80.
- 37) Orłowski RZ, Stinchcombe TE, Mitchell BS, Shea TC, Baldwin AS, Stahl S, et al. Phase I trial of the proteasome inhibitor PS-341 in patients with refractory hematologic malignancies. *J Clin Oncol*. 2002; 20: 4420-7.
- 38) Ohkawa K, Asakura T, Aoki K, Shibata S, Minami J, Fujiwara C, et al. Establishment and some characteristics of epoxomicin (a proteasome inhibitor) resistant variants of the human squamous cell carcinoma cell line, A431. *Int J Oncol*. 2004; 24: 425-33.
- 39) Cai J, Tian AX, Wang QS, Kong PZ, Du X, Li XQ, et al. FOXF2 suppresses the FOXC2-mediated epithelial-mesenchymal transition and multidrug resistance of basal-like breast cancer. *Cancer Lett*. 2015; 367: 129-37.
- 40) Hashida S, Yamamoto H, Shien K, Miyoshi Y, Ohtsuka T, Suzawa K, et al. Acquisition of cancer stem cell-like properties in non-small cell lung cancer with acquired resistance to afatinib. *Cancer Sci*. 2015; 106: 1377-84.
- 41) Huang J, Li H, Ren G. Epithelial-mesenchymal transition and drug resistance in breast cancer (Review). *Int J Oncol*. 2015; 47: 840-8.
- 42) Li H, Zhang P, Sun X, Sun Y, Shi C, Liu H, et al. MicroRNA-181a regulates epithelial-mesenchymal transition by targeting PTEN in drug-resistant lung adenocarcinoma cells. *Int J Oncol*. 2015; 47: 1379-92.
- 43) Liu L, Zhang J, Yang X, Fang C, Xu H, Xi X. SALL4 as an Epithelial-Mesenchymal Transition and Drug Resistance Inducer through the Regulation of c-Myc in Endometrial Cancer. *PLoS One*. 2015; 10: e0138515.
- 44) Piskareva O, Harvey H, Nolan J, Conlon R, Alcock L, Buckley P, et al. The development of cisplatin resistance in neuroblastoma is accompanied by epithelial to mesenchymal transition in vitro. *Cancer Lett*. 2015; 364: 142-55.
- 45) Yang J, Qin G, Luo M, Chen J, Zhang Q, Li L, et al. Reciprocal positive regulation between Cx26 and PI3K/Akt pathway confers acquired gefitinib resistance in NSCLC cells via GJIC-independent induction of EMT. *Cell Death Dis*. 2015; 6: e1829.
- 46) Asakura T, Yamaguchi N, Ohkawa K, Yoshida K. Proteasome inhibitor-resistant cells cause EMT-induction via suppression of E-cadherin by miR-200 and ZEB1. *Int J Oncol*. 2015; 46: 2251-60.
- 47) Boldin MP, Goncharov TM, Goltsev YV, Wallach D. Involvement of MACH, a novel MORT1/FADD-interacting protease, in Fas/APO-1 and TNF receptor-induced cell death. *Cell*. 1996; 85: 803-15.
- 48) Muzio M, Chinnaiyan AM, Kischkel FC, O'Rourke K, Shevchenko A, Ni J, et al. FLICE, a novel FADD-homologous ICE/CED-3-like protease, is recruited to the CD95 (Fas/APO-1) death-inducing signaling complex. *Cell*. 1996; 85: 817-27.
- 49) Srinivasula SM, Ahmad M, Fernandes-Alnemri T, Litwack G, Alnemri ES. Molecular ordering of the Fas-apoptotic pathway: the Fas/APO-1 protease Mch5 is a CrmA-inhibitible protease that activates multiple Ced-3/CE-like cysteine proteases. *Proc Natl Acad Sci USA*. 1996; 93: 14486-91.
- 50) Reed JC. Bcl-2 family proteins: regulators of apoptosis and chemoresistance in hematologic malignancies. *Semin Hematol*. 1997; 34: 9-19.
- 51) Zou H, Henzel WJ, Liu X, Lutschg A, Wang X. Apaf-1, a human protein homologous to *C. elegans* CED-4, participates in cytochrome c-dependent activation of caspase-3. *Cell*. 1997; 90: 405-13.
- 52) Srinivasula SM, Ahmad M, Fernandes-Alnemri T, Alnemri ES. Autoactivation of procaspase-9 by Apaf-1-mediated oligomerization. *Mol Cell*. 1998; 1: 949-57.
- 53) Ghibelli L, Coppola S, Fanelli C, Rotilio G, Civitareale P, Scovassi AI, et al. Glutathione depletion causes cytochrome c release even in the absence of cell commitment to apoptosis. *FASEB J*. 1999; 13: 2031-6.
- 54) Zou H, Li Y, Liu X, Wang X. An APAF-1 cytochrome c multimeric complex is a functional apoptosome that activates procaspase-9. *J Biol Chem*. 1999; 274: 11549-56.
- 55) Gao G, Dou QP. N-terminal cleavage of Bax by calpain generates a potent proapoptotic 18-kDa fragment that promotes Bcl-2-independent cytochrome c release and apoptotic cell death. *J Cell Biochem*. 2000; 80: 53-72.
- 56) Shiraishi H, Okamoto H, Yoshimura A, Yoshida H. ER stress-induced apoptosis and caspase-12 activation occurs downstream of mitochondrial apoptosis involving Apaf-1. *J Cell Sci*. 2006; 119: 3958-66.
- 57) Yokoyama M, Okano T, Sakurai Y, Fukushima S, Okamoto K, Kataoka K. Selective Delivery of Adiramycin to a Solid Tumor Using a Polymeric Micelle Carrier System. *J Drug Targeting*. 1999; 7: 171-86.
- 58) Yokoyama M. Polymeric micelles as a new drug carrier system and their required considerations for clinical trials. *Expert Opin Drug Deliv*. 2010; 7: 145-58.
- 59) Ishibashi Y, Matsumoto T, Niwa M, Suzuki Y, Omura N, Hanyu N, et al. CD147 and matrix metalloproteinase-2 protein expression as significant prognostic factors in esophageal squamous cell carcinoma. *Cancer*. 2004; 101: 1994-2000.

- 60) Tang Y, Nakada MT, Kesavan P, McCabe F, Millar H, Rafferty P, et al. Extracellular matrix metalloproteinase inducer stimulates tumor angiogenesis by elevating vascular endothelial cell growth factor and matrix metalloproteinases. *Cancer Res.* 2005; 65: 3193-9.
- 61) Yan L, Zucker S and Toole BP. Roles of multifunctional glycoprotein, emmprin (basigin; CD147), in tumour progression. *Thromb Haemost.* 2005; 93: 199-204.
- 62) Mamori S, Nagatsuma K, Matsuura T, Ohkawa K, Hano H, Fukunaga M, et al. Useful detection of CD147 (EMMPRIN) for pathological diagnosis of early hepatocellular carcinoma in needle biopsy samples. *World J Gastroenterol.* 2007; 13: 2913-7.
- 63) Ueda K, Yamada K, Urashima M, Ishibashi Y, Shirai M, Nikaido T, et al. Association of extracellular matrix metalloproteinase inducer in endometrial carcinoma with patient outcomes and clinicopathogenesis using monoclonal antibody 12C3. *Oncol Rep.* 2007; 17: 731-5.
- 64) Matsudaira H, Asakura T, Aoki K, Searashi Y, Matsuura T, Nakajima H, et al. Target chemotherapy of anti-CD147 antibody-labeled liposome encapsulated GSH-DXR conjugate on CD147 highly expressed carcinoma cells. *Int J Oncol.* 2010; 36: 77-83.
- 65) Ueda K, Yamada K, Kiyokawa T, Iida Y, Nagata C, Hamada T, et al. Pilot study of CD147 protein expression in epithelial ovarian cancer using monoclonal antibody 12C3. *J Obstet Gynaecol Res.* 2012; 38: 1211-9.
- 66) Lee DH, Goldberg AL. Proteasome inhibitors: Valuable new tools for cell biologists. *Trends Cell Biol.* 1998; 8: 397-403.
- 67) Adams J, Palombella VJ, Sausville EA, Johnson J, Destree A, Lazarus DD, et al. Proteasome inhibitors: A novel class of potent and effective antitumor agents. *Cancer Res.* 1999; 59: 2615-22.
- 68) Meng L, Mohan R, Kwok BH, Eloffson M, Sin N, Crews CM. Epoxomicin, a potent and selective proteasome inhibitor, exhibits in vivo antiinflammatory activity. *Proc Natl Acad Sci USA.* 1999; 96: 10403-8.
- 69) Hideshima T, Richardson P, Chauhan D, Palombella VJ, Elliott PJ, Adams J, et al. The proteasome inhibitor PS-341 inhibits growth, induces apoptosis, and overcomes drug resistance in human multiple myeloma cells. *Cancer Res.* 2001; 61: 3071-6.
- 70) Adams J. Preclinical and clinical evaluation of proteasome inhibitor PS-341 for the treatment of cancer. *Curr Opin Chem Biol.* 2002; 6: 493-500.
- 71) Adams J. Proteasome inhibitors as new anticancer drugs. *Curr Opin Oncol.* 2002; 14: 628-34.
- 72) Almond JB, Cohen GM. The proteasome: A novel target for cancer chemotherapy. *Leukemia.* 2002; 16: 433-43.
- 73) Garber K. On the eve of protein destruction: Ubiquitin research begins to pay off. *J Natl Cancer Inst.* 2002; 94: 550-2.
- 74) Hernandez AA, Roush WR. Recent advances in the synthesis, design and selection of cysteine protease inhibitors. *Curr Opin Chem Biol.* 2002; 6: 459-65.
- 75) LeBlanc R, Catley LP, Hideshima T, Lentzsch S, Mitsiades CS, Mitsiades N, et al. Proteasome inhibitor PS-341 inhibits human myeloma cell growth in vivo and prolongs survival in a murine model. *Cancer Res.* 2002; 62: 4996-5000.
- 76) Ling YH, Liebes L, Ng B, Buckley M, Elliott PJ, Adams J, et al. PS-341, a novel proteasome inhibitor, induces Bcl-2 phosphorylation and cleavage in association with G2-M phase arrest and apoptosis. *Mol Cancer Ther.* 2002; 1: 841-9.
- 77) Sakamoto KM. Ubiquitin-dependent proteolysis: Its role in human diseases and the design of therapeutic strategies. *Mol Genet Metab.* 2002; 77: 44-56.
- 78) Shah SA, Potter MW, Callery MP. Ubiquitin proteasome inhibition and cancer therapy. *Surgery.* 2002; 131: 595-600.
- 79) Smith DM, Wang Z, Kazi A, Li LH, Chan TH, Dou QP. Synthetic analogs of green tea polyphenols as proteasome inhibitors. *Mol Med.* 2002; 8: 382-92.
- 80) Yu R, Ren SG, Melmed S. Proteasome inhibitors induce apoptosis in growth hormone- and prolactin-secreting rat pituitary tumor cells. *J Endocrinol.* 2002; 174: 379-86.
- 81) Esquela-Kerscher A, Slack FJ. Oncomirs - microRNAs with a role in cancer. *Nat Rev Cancer.* 2006; 6: 259-69.
- 82) Berx G, Raspé E, Christofori G, Thiery JP, Sleeman JP. Pre-EMTing metastasis? Recapitulation of morphogenetic processes in cancer. *Clin Exp Metastasis.* 2007; 24: 587-97.
- 83) Burk U, Schubert J, Wellner U, Schmalhofer O, Vincan E, Spaderna S, et al. A reciprocal repression between ZEB1 and members of the miR-200 family promotes EMT and invasion in cancer cells. *EMBO Rep.* 2008; 9: 582-9.
- 84) Korpai M, Kang Y. The emerging role of miR-200 family of microRNAs in epithelial-mesenchymal transition and cancer metastasis. *RNA Biol.* 2008; 5: 115-9.
- 85) Korpai M, Lee ES, Hu G, Kang Y. The miR-200 family inhibits epithelial-mesenchymal transition and cancer cell migration by direct targeting of E-cadherin transcriptional repressors ZEB1 and ZEB2. *J Biol Chem.* 2008; 283: 14910-4.
- 86) Park SM, Gaur AB, Lengyel E, Peter ME. The miR-200 family determines the epithelial phenotype of cancer cells by targeting the E-cadherin repressors ZEB1 and ZEB2. *Genes Dev.* 2008; 22: 894-907.

- 87) Peter ME. Let-7 and miR-200 microRNAs: Guardians against pluripotency and cancer progression. *Cell Cycle*. 2009; 8: 843-52.
- 88) Spaderna S, Brabletz T, Opitz OG. The miR-200 family: central player for gain and loss of the epithelial phenotype. *Gastroenterology*. 2009; 136: 1835-7.
- 89) Gregory PA, Bert AG, Paterson EL, Barry SC, Tsykin A, Farshid G, et al. The miR-200 family and miR-205 regulate epithelial to mesenchymal transition by targeting ZEB1 and SIP1. *Nat Cell Biol*. 2008; 10: 593-601.
- 90) Huang HN, Chen SY, Hwang SM, et al. miR-200c and GATA binding protein 4 regulate human embryonic stem cell renewal and differentiation. *Stem Cell Res (Amst)*. 2014; 12: 338-53.